[1] J. R. Heath, P. J. Kuekes, G. S. Snider, R. S. Williams, *Science* **1998**, *280*, 1716.
[2] K. M. Roth, J. S. Lindsey, D. F. Bocian, W. G. Kuhr, *Langmuir* **2002**, *18*, 4030.
[3] J. Chen, M. A. Reed, *Chem. Phys.* **2002**, *281*, 127.
[4] Y. Chen, J. Jung, D. Ohlberg, X. Li, D. R. Stewart, J. O. Jeppesen, K. A. Nielson, J. Stoddart, R. S. Williams, *Nanotechnology* **2003**, *14*, 462.
[5] Q. Li, G. Mathur, M. Homsi, S. Surthi, V. Misra, V. Malinovskii, K.-H. Schweikart, L. Yu, J. S. Lindsey, Z. Liu, R. B. Dabke, A. Yasseri, D. F. Bocian, W. G. Kuhr, *Appl. Phys. Lett.* **2002**, *81*, 1494.
[6] Q. Li, S. Surthi, G. Mathur, S. Gowda, T. A. Sorenson, R. C. Tenent, W. G. Kuhr, S.-I. Tamaru, J. S. Lindsey, Z. Liu, D. F. Bocian, V. Misra, *Appl. Phys. Lett.* **2003**, *83*, 198.
[7] K. M. Roth, J. S. Lindsey, D. F. Bocian, W. G. Kuhr, *Langmuir* **2002**, *18*, 4030.
[8] K. M. Roth, A. A. Yasseri, Z. Liu, R. B. Dabke, V. Malinovskii, K. Schweikart, L. Yu, H. Tiznado, F. Zaera, J. S. Lindsey, W. G. Kuhr, D. F. Bocian, *J. Am. Chem. Soc.* **2003**, *125*, 505.
[9] D. T. Gryko, F. Zhao, A. A. Yasseri, K. M. Roth, D. F. Bocian, W. G. Kuhr, J. S. Lindsey, *J. Org. Chem.* **2000**, *65*, 7356.
[10] I. Willner, B. Willner, *Pure Appl. Chem.* **2001**, *73*, 535.
[11] Y. Kashiwagi, K. Uchiyama, F. Kurashima, J. Anzai, T. Osa, *Anal. Sci.* **1999**, *15*, 907.
[12] D. M. Collard, M. A. Fox, *Langmuir* **1991**, *7*, 1192.
[13] A. E. Kasmi, J. M. Wallace, E. F. Bowden, S. M. Binet, R. J. Linderman, *J. Am. Chem. Soc.* **1998**, *120*, 225.
[14] H. Imahori, H. Norieda, H. Yamada, Y. Nishimura, I. Yamazaki, Y. Sakata, S. Fukuzumi, *J. Am. Chem. Soc.* **2001**, *123*, 100.
[15] J. Xu, C. Wang, H. Chen, *Anal. Sci.* **2000**, *16*, 231.
[16] H. Kuramitz, K. Sugawara, M. Kawasaki, K. Hasebe, H. Nakamura, S. Tanaka, *Anal. Sci.* **1999**, *15*, 589.
[17] A. J. Bard, L. R. Faulkner, *Electrochemical Methods: Fundamentals and Applications*, John Wiley & Sons, New York **1980**, Ch. 10.7.
[18] D. Gryko, J. Li, J. R. Diers, K. M. Roth, D. F. Bocian, W. G. Kuhr, J. S. Lindsey, *J. Mater. Chem.* **2001**, *11*, 1162.
[19] L. H. Dubois, R. G. Nuzzo, *Annu. Rev. Phys. Chem.* **1992**, *43*, 437.
[20] C. H. Choi, D.-J. Liu, J. W. Evans, M. S. Gordon, *J. Am. Chem. Soc.* **2002**, *124*, 8730.

Magnetic-Field-Induced Growth of Single-Crystalline Fe_3O_4 Nanowires**

By *Jun Wang*, *Qianwang Chen*,* *Chuan Zeng*, and *Binyang Hou*

In the past decade, considerable attention has been drawn towards one-dimensional (1D) nanostructured materials, including nanotubes,[1] nanorods,[2] and nanowires,[3] because of both their interesting physical properties and their wide range of potential applications in nanodevices.[4,5] Much effort has been made to understand the magnetic,[6] electronic,[7] and optical[8] properties of these nanostructures because they exhibit novel physical and chemical properties, differing from those of their bulk counterparts, due to their reduced size and large surface-to-volume ratios.

To date, various approaches have been developed for the preparation of 1D magnetic materials such as magnetic metals, alloys, and metal oxides. For example, a hard-template process such as that using the anodic aluminum oxide (AAO) template is an effective approach for electrochemical deposition of metals and alloys.[9–12] However, the process tends to yield polycrystalline nanowires. Soft-template (lecithin)[13,14] and redox methods,[15–18] on the other hand, can easily lead to the formation of acicular particles. So far, a process for preparation of single-crystalline nanowires of magnetic materials is still lacking. For example, to the best of our knowledge, single-crystalline Fe_3O_4 nanowires have not been reported in the literature. It is known that magnetic materials possess easy magnetic axes. Fe_3O_4, for example, has easy magnetic axes along the [111] and [110] directions.[19] Therefore, an applied external magnetic field might induce oriented growth, for example along the easy magnetic axis, which could result in the formation of 1D nanostructures of magnetic materials. However, no significant oriented growth, especially 1D growth, was observed in approaches with an induced magnetic field.[20–24] For example, only arborescent aggregates were obtained in electrochemical growth of iron under a 0.6 T magnetic field.[20] One-dimensional structure is indeed a product of oriented growth of materials, determined by its growth character and complex experimental conditions such as temperature, pressure, and addition of surfactant. Therefore, experimental conditions need to be carefully selected and well controlled to show the effect of magnetic field on the growth of magnetic materials. So far, little attention has been paid to the crystallization behavior of magnetic materials in an aqueous system under an external magnetic field. In this communication, we report the preparation of ferromagnetic Fe_3O_4 nanowires by a hydrothermal process with an external magnetic field applied.

As shown in Figure 1, the sample formed under a magnetic field is pure Fe_3O_4 without any impurity phases. Mössbauer spectrum analysis was also carried out to confirm the formation of Fe_3O_4. The spectrum (not shown) consists of two hyperfine magnetic sextets (H_{hf}: 49.22 T and 46.02 T), one for the Fe^{3+} tetrahedral site and the other for the mixed valence $Fe^{2.5+}$ octahedral site. This result also shows that the sample is not γ-Fe_2O_3 but Fe_3O_4.[25,26] In Figure 1, the broadening of reflection peaks is obvious, which indicates the formation of ultrafine particles. It was also found that the weak peak (422) became as strong as the peak (511), which might originate from the growing orientation of particles.

Figure 2 shows transmission electron spectroscopy (TEM) images of representative samples prepared under external magnetic fields, which clearly reveal the effect of magnetic field on the nucleation and growth process of Fe_3O_4. Without a magnetic field applied, Fe_3O_4 particles (50 nm) are square

[*] Prof. Q. Chen, Dr. J. Wang, C. Zeng, B. Hou
Structure Research Laboratory and
Department of Materials Science and Engineering
University of Science and Technology of China
Hefei 230026 (P.R. China)
E-mail: cqw@ustc.edu.cn

[**] This work was supported by the National Natural Science Foundation under contract no. 20125103 and no. 90206034.

 DOI: 10.1002/adma.200306136

ADVANCED MATERIALS

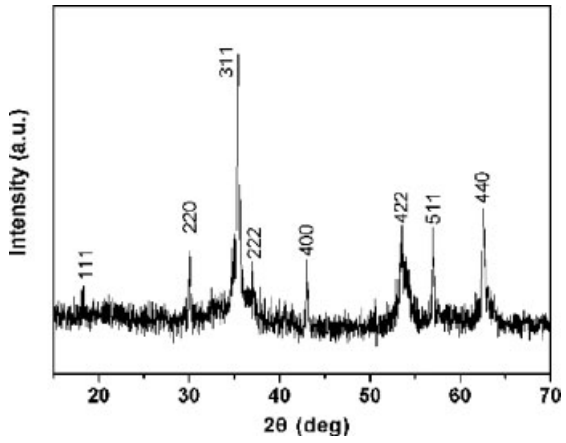

Figure 1. XRD pattern of the sample prepared under a 0.25 T magnetic field.

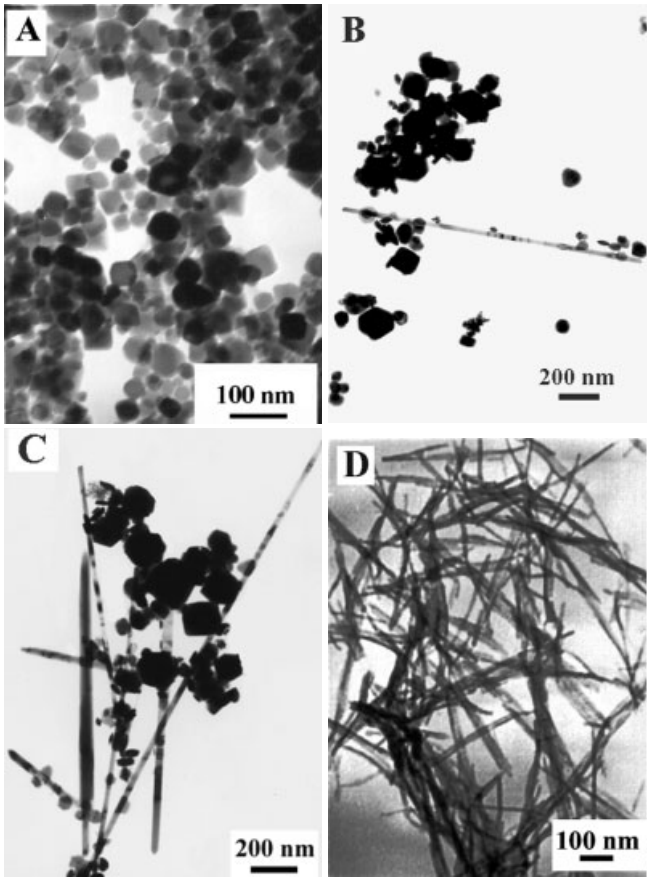

Figure 2. TEM images of the samples obtained in zero magnetic field (A), and 0.15 T (B), 0.25 T (C), and 0.35 T (D) magnetic fields.

and hexagonal in shape (Fig. 2A). Interestingly, the morphology changed drastically when an external magnetic field was applied. In addition to square particles, nanowires were observed in the sample when a 0.15 T magnetic field was applied (Fig. 2B). When the strength of the magnetic field was increased to 0.25 T, the ratio of the nanowires to square particles was about 2:3, as estimated from the TEM image (Fig. 2C). When the strength reached 0.35 T, the morphology of Fe_3O_4 changed again: a large number of nanowires and a fibrous nanostructure of Fe_3O_4 formed (diameter 20 nm and length about 0.8 μm), accompanied by the disappearance of the square particles (Fig. 2D). The results clearly show that the external magnetic field could be responsible for the formation of nanowires and nanofibers in large quantities.

When a 0.25 T magnetic field was applied, the diameter and length of the typical nanowires were 35–100 nm and 0.48–2.7 μm, respectively (Fig. 2C). A representative TEM image of a Fe_3O_4 nanowire is shown in Figure 3A. The electron diffraction (ED) pattern (the inset of Fig. 3A) obtained along a typical individual nanowire confirms the Fe_3O_4 nanowire to

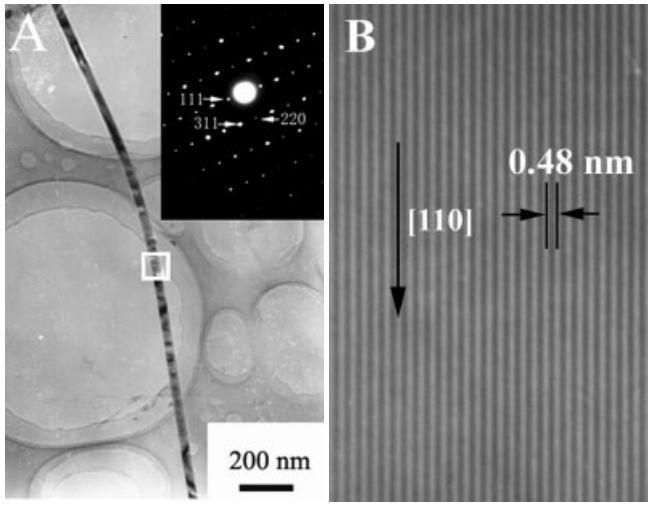

Figure 3. Representative TEM image of a typical Fe_3O_4 nanowire (A); the inset in (A) shows an ED pattern of the individual Fe_3O_4 nanowire. B) HRTEM image of the nanowire (boxed area in (A)). The Fe_3O_4 nanowire was prepared under a 0.25 T magnetic field.

be single crystalline. The high-resolution transmission electron microscopy (HRTEM) image of the boxed area in Figure 3A further supports the single-crystalline nature of these Fe_3O_4 nanowires (Fig. 3B). The lattice fringes (~0.48 nm) observed in this image agree well with the separation between the (111) lattice planes. Combined with the ED results it is confirmed that the nanowires grew along [110], one of the easy magnetic axes of Fe_3O_4.

It seems that the Lorentz force plays a role at the level of individual ions in the aqueous solution, inducing the preferential nucleation and growth of Fe_3O_4. Possibly the surface tension anisotropy is imposed in Fe_3O_4 crystal growth and the morphology symmetry breaking is induced by the extra magnetic field associated with nanowires. A detailed analysis of magnetic effects is complex due to the lack of in situ observation results. Nevertheless, we can conclude that magnetic fields could induce nanowire growth along the easy magnetic axis of Fe_3O_4 in aqueous solution.

As mentioned above, beside nanowires some square and hexagonal particles were also formed in the reaction under 0.15 and 0.25 T magnetic fields (Fig. 2B,C), which is quite similar to what is formed in a hydrothermal process without a magnetic field. In the reaction cell with a 0.25 T permanent magnet installed in its bottom, the strength of the magnetic field measured by a Tesla meter decreases from the lower inner surface (0.25 T) to the top surface (0.04 T) in the cell. The nucleation and growth of Fe_3O_4 take place in the areas with weaker magnetic field strength, such as the area near the top surface, which would result in the formation of square and hexagonal particles rather than nanowires. To verify the above speculations, a similar reaction was carried out in a cell with a magnetic field of 0.15 T applied. TEM studies show that the yield of Fe_3O_4 nanowires decreases significantly compared with that under an external magnetic field of 0.25 T, which reveals that the magnetic field is the source of the wire-like growth of Fe_3O_4 particles and the yield depends on the strength of the magnetic field applied. It is expected that more interesting results would be obtained if the strength of the magnetic field could be adjusted continuously.

Figure 4 shows magnetic hysteresis curves for the samples measured at room temperature. It shows that sample B (mixture of particles and nanowires) (0.25 T, Fig. 4B) and sample C (nanowires and fibrous nanostructure) (0.35 T, Fig. 4C)

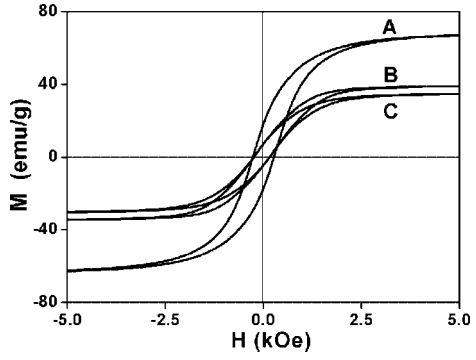

Figure 4. Magnetic hysteresis curves measured at room temperature for the samples prepared by a hydrothermal process with zero (A), 0.25 T (B), and 0.35 T (C) magnetic field applied.

have saturation magnetization of 39.5 emu/g and 35.2 emu/g, respectively. Both of them are lower than the 68.7 emu/g of sample A (Fig. 4A). Although the source of low saturation magnetization is not clear, the high shape anisotropy of the nanowires, preventing them from magnetizing in directions other than along their easy magnetic axes, might be a major reason. With a random orientation of nanowires, the projection of the magnetization vectors along the field direction will be lower than that for a collection of nanoparticles without the large shape anisotropy effect. On the other hand, pinning of the magnetic domains in Fe_3O_4 nanowires might also be responsible for the low saturation magnetization. Magnetic domains in the nanowires are oriented parallel, perpendicular, and even antiparallel to the measured magnetic field. The diameters of the nanowires are around the critical size (54 nm) of Fe_3O_4 single domains.[27] The antiparallel magnetic domains, for example, must overcome much higher energy barriers to align in the direction relative to the measured magnetic field due to the spatial confinement effect in the direction perpendicular to the nanowires. Further work should be done to clarify the physical origin completely.

In conclusion, it is observed that an external magnetic field can significantly influence the growth behavior of nanoparticles formed in a hydrothermal system. Single-crystalline nanowires of Fe_3O_4 with diameters of 35–100 nm and lengths of about 0.48–2.7 μm were formed under a 0.25 T magnetic field; increasing the strength of the magnetic field can increase the yield of nanowires, while square and hexagonal particles are formed under zero magnetic field. HRTEM and ED results confirm that the single-crystalline nanowires grow along [110], showing that the external magnetic field results in growth of Fe_3O_4 nanowires along one of its easy magnetic axes. However, only a lower saturation magnetization was observed in the sample, which was explained in terms of the pinning of antiparallel magnetic domains in Fe_3O_4 nanowires due to the spatial confinement effect and the high shape anisotropy of the nanowires, which prevents them from magnetizing in directions other than along their axes. It is expected that this process could be a promising technique to synthesize 1D nanostructures of other magnetic materials.

Experimental

The reaction cells were self-made with permanent magnets under a Teflon (poly(tetrafluoroethylene)) lining. The strengths of the magnetic fields on the inner lower surface of the cells were 0, 0.15 T, 0.25 T, and 0.35 T, respectively. The chemical reagents used were ferrous chloride ($FeCl_2{\cdot}4H_2O$), sodium hydroxide (NaOH), and diamine hydrate ($H_4N_2{\cdot}H_2O$, 50 % water). All the chemicals were of analytical grade. Distilled water, degassed with N_2 gas for half an hour, was used for the preparation of an aqueous solution of Fe^{2+} ions (0.1 mol/L). Fe^{2+} solution (30 mL) was put into a Teflon-lined stainless autoclave, and sodium hydroxide (0.6 g) was dissolved into $H_4N_2{\cdot}H_2O$ (5 mL) and then the mixture was slowly dropped into the autoclave. During the experiment, N_2 was continuously passed through the solution to prevent the oxidation of Fe^{2+} in the system. The autoclave was put into an oven, kept at 130 °C for 6 h, and then cooled to room temperature naturally. The products were filtered and washed several times with distilled water and absolute ethanol, and finally dried in vacuum oven at 25 °C for 12 h. All the other parameters were fixed as the strength of the magnetic field changed.

X-ray diffraction was performed on a Rigaku X-ray diffractometer with high-strength Cu Kα radiation. TEM images were taken with a Hitachi model H-800 transmission electron microscope, using an accelerating voltage of 200 kV. HRTEM images were taken on JEOL-2010 high-resolution electronic microscope with an accelerating voltage of 200 kV. Their magnetic properties were evaluated on a BHV-55 V.S. vibrating sample magnetometer (VSM), and the field reached up to 0.5 T.

Received: July 31, 2003
Final version: September 8, 2003

ADVANCED MATERIALS

[1] J. T. Hu, T. W. Odom, C. M. Lieber, *Acc. Chem. Res.* **1999**, *32*, 435.
[2] V. F. Puntes, K. M. Krishnan, A. P. Alivisatos, *Science* **2001**, *291*, 2115.
[3] J. D. Holmes, K. P. Johnstin, R. C. Doty, B. A. Korgel, *Science* **2000**, *287*, 1471.
[4] J. F. Wang, M. S. Gudiksen, X. F. Duan, Y. Cui, C. M. Lieber, *Science* **2001**, *293*, 1445.
[5] H. Kind, H. Q. Yan, B. Messer, M. Law, P. D. Yang, *Adv. Mater.* **2002**, *14*, 158.
[6] T. Thurn-Albrecht, J. Schotter, C. A. Kastle, N. Emley, T. Shibauchi, L. Krusin-Elbaum, K. Guarini, C. T. Black, M. T. Tuominen, T. P. Russell, *Science* **2000**, *290*, 2126.
[7] W. J. Liang, M. Bockrath, D. Bozovic, J. H. Hafner, M. Tinkham, H. Park, *Nature* **2001**, *411*, 665.
[8] X. F. Duan, Y. Huang, Y. Cui, J. Wang, C. M. Lieber, *Nature* **2001**, *409*, 6816.
[9] M. Tanase, D. M. Silevitch, A. Hultgren, L. A. Bauer, P. C. Searson, G. J. Meyer, D. H. Reich, *J. Appl. Phys.* **2002**, *91*, 8549.
[10] S. H. Ge, C. Li, X. Ma, W. Li, L. Xi, C. X. Li, *J. Appl. Phys.* **2001**, *90*, 509.
[11] S. G. Yang, H. Zhu, D. L. Yu, Z. Q. Jin, S. L. Tang, Y. W. Du, *J. Magn. Magn. Mater.* **2000**, *222*, 97.
[12] H. R. Khan, K. Petrikowski, *Mater. Sci. Eng. C* **2002**, *19*, 345.
[13] J. L. Cain, D. E. Nikles, *IEEE Trans. Magn.* **1997**, *33*, 3718.
[14] M. Chen, D. E. Nikles, *J. Appl. Phys.* **1999**, *85*, 5540.
[15] C. Sudakar, G. N. Subbanna, T. R. N. Kutty, *J. Mater. Chem.* **2002**, *12*, 107.
[16] H. Kurokawa, M. Senna. *Powder Technol.* **1999**, *103*, 71.
[17] D. Concepcion, R. Rapael, B. J. Miguel, *J. Colloid Interface Sci.* **1994**, *165*, 244.
[18] K. Kandori, M. Fukuoka, T. Ishikawa, *J. Mater. Sci.* **1991**, *26*, 3313.
[19] Y. L. Li, G. D. Li, *Physics of Ferrite*, Science Publishing Corporation, Beijing **1978**, p. 381.
[20] S. Boden, L. Vignon, M. R. P. Ballou, *Phys. Rev. Lett.* **1999**, *83*, 2612.
[21] Y. W. Ma, K. Watanabe, S. S. Awaji, M. Motokawa, *J. Cryst. Growth* **2001**, *233*, 483.
[22] S. H. Ge, C. Li, X. Ma, W. Li, C. X. Li, *Acta Phys. Sin.* **2001**, *50*, 149.
[23] R. Oshima, H. Tokoro, *J. Jpn. Inst. Met.* **1998**, *62*, 317.
[24] H. Yokomichi, S. Hiroyuki, *Appl. Phys. Lett.* **1999**, *74*, 1827.
[25] R. Bauminger, S. G. Cohen, A. Marinov, S. Ofer, E. Segal, *Phys. Rev.* **1961**, *122*, 1447.
[26] S. K. Banerjee, W. O'Reilly, *J. Appl. Phys.* **1967**, *38*, 1289.
[27] A. Aharoni, J. P. Jakubovics, *IEEE Trans. Magn.* **1988**, *24*, 1892.

Rational Design of Macrocellular Silica Scaffolds Obtained by a Tunable Sol–Gel Foaming Process

By *Florent Carn*, *Annie Colin*,* *Marie-France Achard*, *Hervé Deleuze*, *Zoubida Saadi*, and *Rénal Backov**

By considering the extraordinary number of shapes of hierarchically organized materials that exist in nature, researchers, including chemists, physicists, and biologists, are striving to reproduce those morphologies in the laboratory. Their efforts have led to the ever-growing field of so-called "bio-inspired" materials.[1–5] While micro- and mesoscale void-space texturation is a rather well established method today,[6–11] supermeso- or macroscale morphosynthesis (i.e., pore sizes > 50 nm) is a more recent development.[12–16] Thus, monolith-type materials with hierarchical porosity attract considerable attention due to their wide scope of applications.[17,18] In the context briefly described above, Bagshaw, using metastable non-ionic surfactant air–liquid foams induced by strong stirring, was able to achieve void spaces with a high polydispersity of 200–500 μm and random shapes.[19] It was claimed that the macroscale morphologies were tuned by changing the turbulence of the reaction media, which is certainly a very difficult parameter to control. However, even if the final monolith-type materials appear strongly inhomogeneous at the macroscopic level, this method has the double advantage of simplicity and low cost. In this study, we present an alternative method which makes use of a bubbling process to produce air–liquid foams. This method allows complete control over the cell sizes and shapes of the bubbles and a more facile tunability of the liquid fraction of the foam. In addition, the macroscale morphology of the silica scaffolds can be controlled by the pore size of the glass disk employed during the bubbling process. Further, the final monolith-type materials possess meso- and macroscale hierarchically organized void spaces where, for the first time, the macroscale inorganic-polymer morphologies (i.e., length, width, and curvature of the Plateau borders) can be tuned almost on demand. In order to both fully mineralize the Plateau borders of the foam and assure mesoporosity, the methodology described here is not based on the common ceramic processing technique. Usually, slurry mixing of organic polymer fibers with an inorganic powder is followed by thermal treatment allowing removal of the organic polymer core. Instead, we induced silica condensation within the macroscale confining media of the air–liquid foam. As the foam is a metastable system, and as the sol–gel process and the foam preparation require antagonistic experimental conditions, a rigorous and careful synthetic procedure must be applied. First, because alcohol is a poison to foam, most of the ethanol produced by the hydrolysis of tetraethylorthosilicate (TEOS) must be evaporated before beginning the bubbling process. We thus started the bubbling process when the TEOS hydrolysis was finished. Second, during the foam production we were able to produce foam with calibrated bubble sizes. To achieve this, we chose the pH range carefully in order to obtain a medium aggregation kinetic of the nanoparticles while minimizing the viscosity of the aqueous media. Third, as the foam must be stable during the sol–gel process, a mixture of gases (perfluorohexane and nitrogen) was employed to limit Ostwald ripening. Additionally, to overcome coalescence of the bubbles, we made use of a cationic surfactant.[20] The major cause of destabilization in such foams is drainage, i.e., the flow of the liquid between the bubbles due to gravity. In order to minimize this phenomenon, we wet the foam from above with

[*] Dr. R. Backov, Dr. A. Colin, F. Carn, Dr. M.-F. Achard, Z. Saadi
Centre de Recherche Paul Pascal
UPR 8641-CNRS, Avenue Albert Schweitzer, F-33600 Pessac (France)
E-mail: backov@crpp-bordeaux.cnrs.fr, colin@crpp-bordeaux.crns.fr
Dr. H. Deleuze
Laboratoire de chimie Organique et Organométallique
UMR 5802-CNRS, Université Bordeaux 1
351 Cours de la Libération, F-33045 Talence Cedex (France)

  DOI: 10.1002/adma.200306067